



Subsalt structure prediction based on the fast 3d salt tectogenesis modeling

B. Lunev, T. Abramov, V. Lapkovsky (IPGG/SB RAS, Russia), V. Priimenko (LENEP/UENF & INCT - GP/CNPq/MEC, Brazil)

Copyright 2017, SBGf - Sociedade Brasileira de Geofísica

This paper was prepared for presentation during the 15th International Congress of the Brazilian Geophysical Society held in Rio de Janeiro, Brazil, 31 July to 3 August, 2017.

Contents of this paper were reviewed by the Technical Committee of the 15th International Congress of the Brazilian Geophysical Society and do not necessarily represent any position of the SBGf, its officers or members. Electronic reproduction or storage of any part of this paper for commercial purposes without the written consent of the Brazilian Geophysical Society is prohibited.

Abstract

There are presented some results of testing a computational program developed for prediction of the geological structures and the stress-strain state in exploration and characterization of the hydrocarbon deposits in the areas of salt tectonics.

Introduction

It is known that salt tectonics largely control the hydrocarbon deposits distribution in many oil/gas bearing provinces. Recently, major interest has been attached to subsalt hydrocarbon prospecting, particularly where the oil source rocks are expected beneath the salt (e.g., in the Caspian region and Gulf of Mexico). The difficulties encountered in geophysical survey of salt diapirs are well known; the well-boring in such regions is connected with even greater problems. In such circumstances, any reasonable forecast of the geological structure and the associated stress-strain state would be useful for an optimal planning of exploration minimizing the associated costs. Numerical modeling of the salt structures evolution targeted to reproducing studied objects may be a good tool in this.

Many scientific studies carried out in this direction, allowed to reveal the basic laws of salt tectogenesis as creeping flow that implements the Rayleigh-Taylor instability. However, the practical use of the numerical modeling was still limited. The point is that the reproduction of a specific geologic formation to simulate the structure requires a large number of alternative models of evolution in order to select the optimal variant in accordance with the valid data. Therefore, an important requirement to the software is its performance.

Unfortunately, existing numerical algorithms based on the finite difference methods require too much computational time to simulate situations similar to real ones - with a large number of complex layers with different physical properties. In this case, parallel computing does not help much: due to inevitable frequent exchange between computing nodes, speed up is limited by memory bandwidth rather than peak performance of devices.

We managed to get around these difficulties and to create high-performance software for calculation of creeping flow, modeling the processes of salt tectogenesis.

Statement of the Problem

In accordance with the formalism of "Theories of simple liquids with fading memory" (Astarita & Marrucci, 1978), the irreversible deformations of almost all material are, within the first approximation, described by the equations of Newtonian fluid rheology. This approximation is suitable for the strain rates below a certain critical value for a given material. The critical strain rate in the rocks is estimated to be about 10^{-14} s^{-1} (Lunev, 1996). At that, the Newtonian viscosity is treated as a "natural" viscosity of the material, defined as the upper asymptote of its viscometric viscosity. The available data (Jackson & Talbot, 1986) show that:

- strain rate does not exceed the mentioned limit in the processes of the growth of a salt dome;
- although the estimates of effective (viscometric) viscosity for sedimentary rocks, especially, salt, widely vary depending on the estimation method and the strain rate, all these rocks have similar upper asymptotes (about $10^{20} \text{ Pa}\cdot\text{s}$);
- characteristic mushroom shape of mature salt domes definitely indicates that the salt and the hosting rocks have similar viscosity values in this process.

Thus, for this class of problems, approximation of the medium as a homogeneous viscous Newtonian fluid is quite reasonable. Anyway, the solutions obtained by this approach, will be true (as a first approximation) regardless of the behavior of the medium in more fast processes.

The fact that the Reynolds number is *a priori* known to be small (about 10^{-22}) and classifies the been studied flow as a "creeping", the evolution of which can be represented by a sequence of interconnected quasi-stationary states. In accordance with these facts, salt tectogenesis can be modeled (in domains bounded above by a free surface) by the gravitational creeping of a Newtonian fluid with inhomogeneous density and constant viscosity.

To formulate our mathematical problem, we consider a half-space $x_3 \leq h(x_1, x_2, t)$, $\mathbf{x} = (x_1, x_2, x_3) \in \mathbf{R}^3$, limited by a free boundary $F(x, t) \equiv x_3 - h(x_1, x_2, t) = 0$. We assume that this half-space is composed by a set of immiscible layers (or closed bodies) D_k , $k = 1, 2, \dots, n$,

separated by boundaries $S_k(\mathbf{x}, t)$, whose configuration is changed by the calculated flow. The flow is driven by normal gravity force \mathbf{g} applied to perturbation of the density, connected with the configuration of boundaries $S_k(\mathbf{x}, t)$. Initial data are defined by some configuration of $S_k(\mathbf{x}, t)$. Density, stresses and pressure are given as follows:

$$\begin{aligned}\rho(\mathbf{x}, t) &= \rho^0(x_3, t) + \sigma(\mathbf{x}, t), \\ \mathbf{T}(\mathbf{x}, t) &= \mathbf{T}^0(x_3, t) + \mathbf{t}(\mathbf{x}, t), \\ P(\mathbf{x}, t) &= P^0(x_3, t) + p(\mathbf{x}, t).\end{aligned}$$

Here \mathbf{T}^0, P^0 are characteristics of the hydrostatic state

$$\mathbf{T}^0 = -P^0 \mathbf{I}, P^0 = -g \int_0^{x_3} \rho^0(\xi, t) d\xi,$$

\mathbf{I} is the 3×3 -identity matrix, $g = |\mathbf{g}|$, and σ, \mathbf{t}, p are their small perturbations; flow $\mathbf{v}(\mathbf{x}, t)$ is associated with these perturbations.

The problem of calculating the creep flow may be formulated as follows.

In the quasi-stationary case, given $\sigma(\mathbf{x}, t^), \mathbf{t}(\mathbf{x}, t^*)$ (t^* is fixed), it is required to find $\mathbf{v}(\mathbf{x}, t^*), p(\mathbf{x}, t^*)$ and the shape of the free boundary $F(\mathbf{x}, t^*)$:*

$$\begin{aligned}\mu \nabla^2 \mathbf{v} - \nabla p &= -\sigma \mathbf{g}, \nabla \cdot \mathbf{v} = 0, \\ \frac{\partial F}{\partial t} + \mathbf{v} \cdot \nabla F &= 0, \\ F: \mathbf{T} \cdot \mathbf{v} = \mathbf{0}, S_k: [\mathbf{v}] = \mathbf{0}, [p] = 0,\end{aligned}\quad (1)$$

where μ is the viscosity, $[\cdot]$ means jump of the corresponding function, and the density is described by a piece-wise constant function, i.e., $\rho(\mathbf{x}, t^*) \equiv \rho_k$ for $\mathbf{x} \in D_k$. The evolutionary problem describing evolution of the internal boundaries S_k is:

$$\begin{aligned}\frac{\partial S_k}{\partial t} + \mathbf{v} \cdot \nabla S_k &= 0, \\ S_k(\mathbf{x}, t_0) &= S_k^0(\mathbf{x}),\end{aligned}\quad (2)$$

where $\mathbf{v}(\mathbf{x}, t_0) = \mathbf{0}$.

The evolution of the flow is calculated by solving problem (1) with $S_k(\mathbf{x}, t^*)$ specified by (2) and the corresponding density perturbation σ , and the subsequent integration of (2) (with just obtained \mathbf{v}) with respect to small time increments δt .

Method

Assuming smallness of the free boundary perturbations (compared to the horizontal scale), we can linearize the quasi-stationary problem (1) obtaining

$$\begin{aligned}\mu \nabla^2 \mathbf{v} - \nabla p &= -\sigma \mathbf{g}, \nabla \cdot \mathbf{v} = 0, \\ x_3 = 0: v_3 = \tau_{31} = \tau_{32} &= 0\end{aligned}\quad (3)$$

with the additional condition for the determination of perturbation of the free surface F :

$$x_3 = 0: \tau_{33} = -\rho^0 g h.\quad (4)$$

The jump conditions in (1) are replaced by the continuity of \mathbf{v}, p everywhere in the considered half-space.

In the case of homogeneous, viscous and incompressible Newtonian fluid the vector Green function $\mathbf{G}(\mathbf{x} - \mathbf{y})$ of the considered problem was obtained analytically (Lunev, 1986). Using this function we can find $\mathbf{v}(\mathbf{x}, t^*), p(\mathbf{x}, t^*)$ in the form of convolution integrals

$$\begin{aligned}\mathbf{v}(\mathbf{x}) &= g \iiint \sigma(\mathbf{y}) \mathbf{G}_v(\mathbf{x} - \mathbf{y}) d\mathbf{y}, \\ p(\mathbf{x}) &= g \iiint \sigma(\mathbf{y}) G_p(\mathbf{x} - \mathbf{y}) d\mathbf{y},\end{aligned}\quad (5)$$

where \mathbf{G}_v, G_p are the corresponding parts of the vector Green function.

The convolution integrals calculation gives great computational advantages in comparison to the solution of a linear system obtained by the finite difference methods. Using the Green function is especially effective in the planning massive parallel computing. As a result, the acceleration is proportional to the peak performance of the system and not to the memory bandwidth. The scalability of problem on an arbitrarily large number of computing nodes is obvious.

Additional acceleration of the calculations permits to calculate the velocity field only at the boundaries of bodies (layers) with different densities, instead of the calculation of the velocity field over the entire region (which would be necessary in the case of finite difference methods). Because of this, in a way, we reduce dimensionality of the problem, calculating the three-dimensional object (density distribution) on the two-dimensional surface only. At the same time, the explicit description of movement of the boundaries increases the accuracy of the total flow calculation.

Explicit form of the Green function gives a possibility to use the convolution theorem and the FFT. In this case, the direct summation is replaced by the multiplication of the Fourier transform of the density function and the Green function with consequent application of the inverse Fourier transform. The flow rate is calculated on the grid and their values on the layer boundaries are obtained by interpolation, which reduces accuracy, compared with the direct summation in the coordinate domain. However, for a sufficiently dense grid, this decline does not matter, and

the computational speed is increased dramatically - an order of magnitude or more. This method is useful for rapid selection of the more confidence version of the evolutionary process, in order to indicate one that reproduces the object of interest. The selected variant can be verified using the direct summation method.

Some of advantages of this method were realized in parallel computing programs, focused on the use of GPU's. In these programs, developed for three-dimensional modeling, we implemented an explicit description of the layer boundaries in the form of triangulated surfaces. At each time step, the grid of sources was restored from the configuration of boundaries (the grid of sources has a fixed size and is more rough approximation of the density field). Such a description, reduced the complexity of the task and at the same time increased the accuracy of the calculations, allowing using single precision instead of double one (tests have shown that using single or double precision gives almost identical results up to the deep stages of evolution). Modern GPU's are characterized by a large difference in performance with single and double precision, so the use of single precision accelerated calculations significantly.

To calculate integrals (5) with help of the parallel computing, we used appropriately modified methods for solving the problem of many bodies interaction, see (Harris et al., 2007). When the convolution theorem was implemented, the direct and inverse Fourier transforms were done with help of the cuFFT library (cuFFT User Guide).

Examples

The programs created allow us to analyze the evolution of Rayleigh - Taylor instability for complex, multi-layered models with superimposed background (from geological considerations) of differentiated dive-uplift movements accompanied by accumulation, compaction and erosion of sediments. For every stage of evolution we can also calculate all the components of the stress-strain state and the corresponding perturbation of the relief surface. The characteristic time of calculation for complex models to the deep stages of the evolution is of the order of 10 minutes - 1 hour. The calculations were performed on a personal computer equipped with a Tesla c1060 and on a single computing cluster node with three Tesla M2090.

The results obtained are in good agreement with ones of physical modeling, Fig.1, and reproduce the formation of real geological structures, see Fig.2. Possibility of investigating the evolution of multi-layer models allowed to obtain some theoretically and practically important results regarding the dynamics and structures of subsalt. It was found that rising of diapirs in suprasalt causes counterflow in subsalt, leading to the development of inversion folding there. So, that suprasalt diapirs correspond to the subsalt synclines while the suprasalt inter-diapir sags correspond to the anticlines in the subsalt. The amplitude of the folds in the upper subsalt layers attains 500 m and more, their length is closed to the wavelength of the perturbation of the upwelling layer.

The most intense folding involves the uppermost 1km subsalt layers. The deformations steeply die out with increasing depth. The cores of the synclines beneath the diapirs are formed due to the swelling of the uppermost subsalt layer, whose top portion is pulled into the diapir. An example of such evolution is shown in Fig.3.

The developed program allows to calculate the evolution of very complex models to deep stages. As an example, in Fig.4 shows the final state of a calculated model, containing two unstable layers.

These results are of particular importance because of the tendency to search for hydrocarbon deposits in the subsalt (the Caspian region, the Atlantic shelf of Africa and South America, and others), where quite similar inversion folds in subsalt were established by modern seismic methods, see, for instance, (Hantschel & Kauerauf, 2009).

Conclusions

There was developed and realized a computational algorithm, which can be a useful tool for prediction of the geological structure and the stress-strain state in exploration and characterization of the hydrocarbon deposits in the salt tectonics areas. The results obtained show a good potential of the developed technique in the solution of corresponding geological tasks.

Acknowledgments

The work was supported by the Siberian Branch of the Russian Academy of Sciences, Program IX.131.2.2.

References

- ASTARITA, G. & MARUCCI, G.** 1974. Principles of Non-Newtonian Fluid Mechanics. New York, Mc Graw-Hill.
- cuFFT User Guide.
<http://docs.nvidia.com/cuda/cufft/index.html>
- HANTSCHEL, T. & KAUEAUF, A.I.** 2009. Fundamentals of Basin and Petroleum Systems Modeling. Berlin, Springer.
- HARRIS, M.; LARS, N.; PRINS, J.** 2007. Fast n-body simulation with CUDA. In: GPU Gems 3. Addison-Wesley, Boston, MA, 677-695.
- JACKSON, M.P.A. & TALBOT, C.J.** 1986. External shapes, strain rates and dynamics of salt structures. Geological Society of America Bulletin, **97**, 305-323.
- LUNEV, B.V.** 1986. Isostasy as dynamical equilibrium of viscous fluid. Dokl. AN USSR, Earth Sci., **290**(1), 72-76.
- LUNEV, B.V.** 1996. On the nature of upper-mantle density anomaly beneath the Mid-Atlantic Ridge and its role in rifting and spreading. Rus. Geol. Geophys., **37**(9), 87-101.
- TALBOT, C.J. & JACKSON, M.P.A.** 1987. Salt tectonic. Scientific American, **257**(2), 70-79.

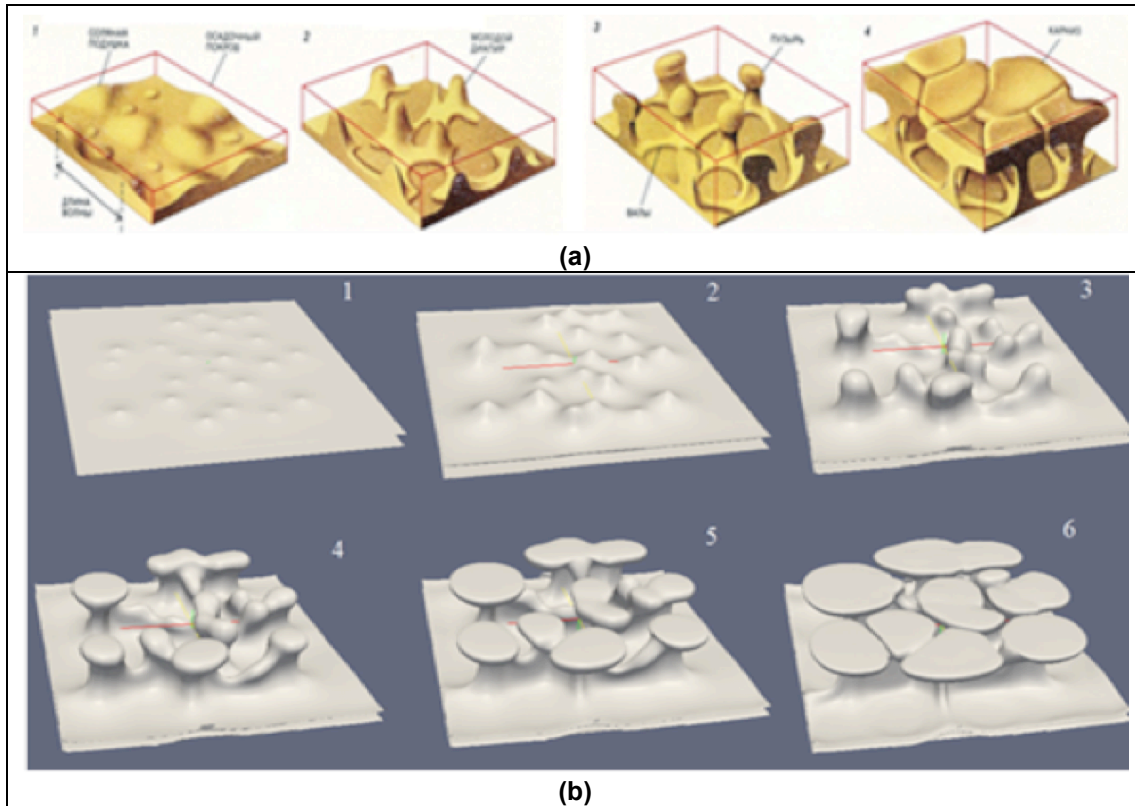


Figure 1 - (a) Results of physical modeling – stages of low-density layer upwelling in a centrifuge (Talbot & Jackson, 1987), and (b) similar sequence calculated in our numerical experiment. Observe a similarity of the results of physical and numerical modeling; the differences are due to the difference of the initial perturbations setting (defined by a random number generator).

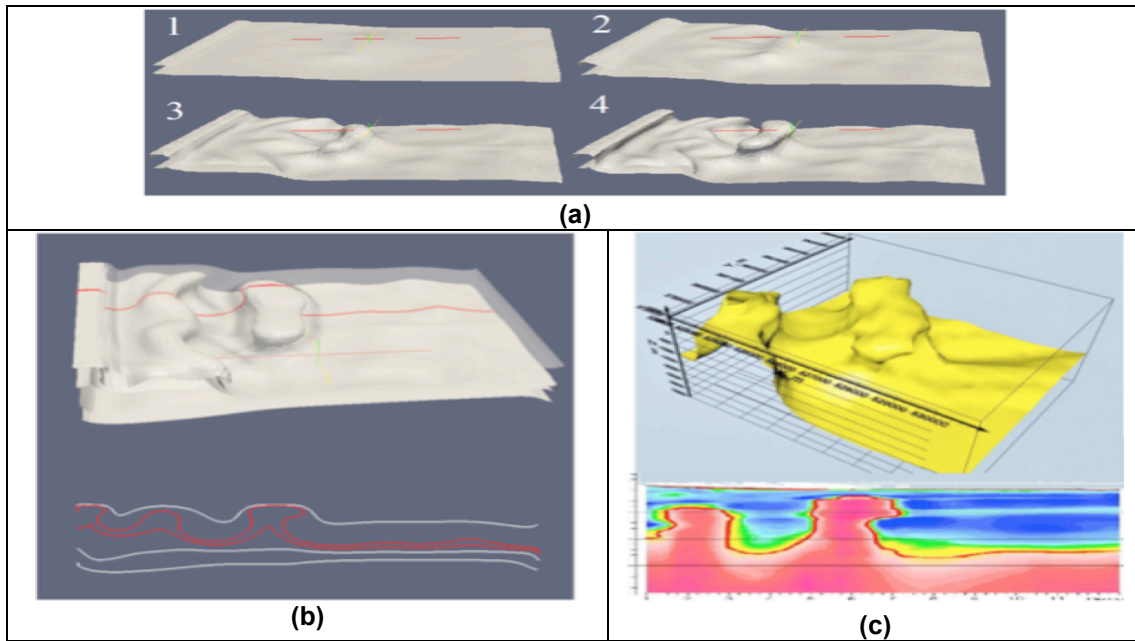


Figure 2 - Real salt diapirs and result of the calculated evolution, which reproduce this structure, (a) sequence of steps of evolution, (b) - final stage of the calculated evolution (surface and cross-section), (c) real structure top of salt and cross-section obtained by geophysical data.

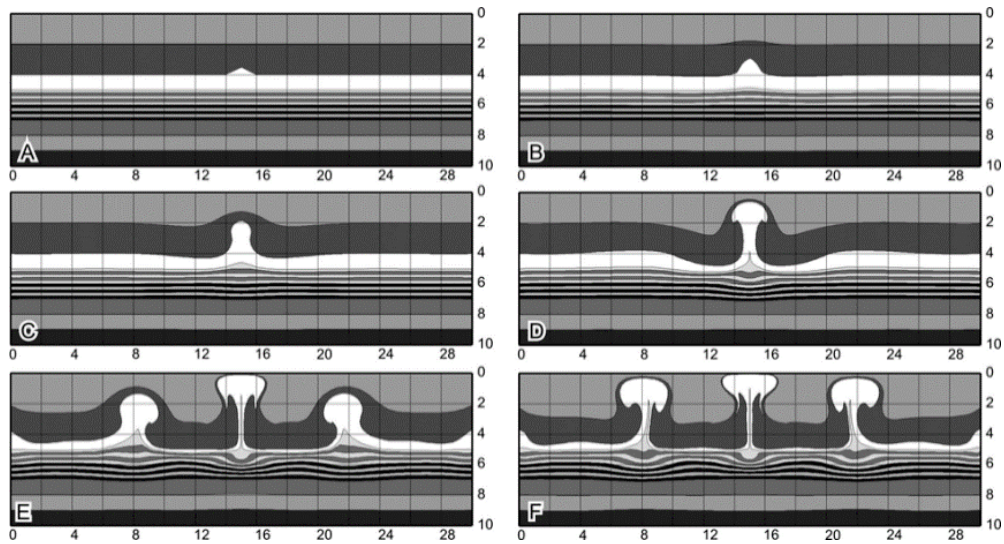


Figure 3 - Stages of the Rayleigh-Taylor instability with formation of the inversion folding below the rising unstable layer.

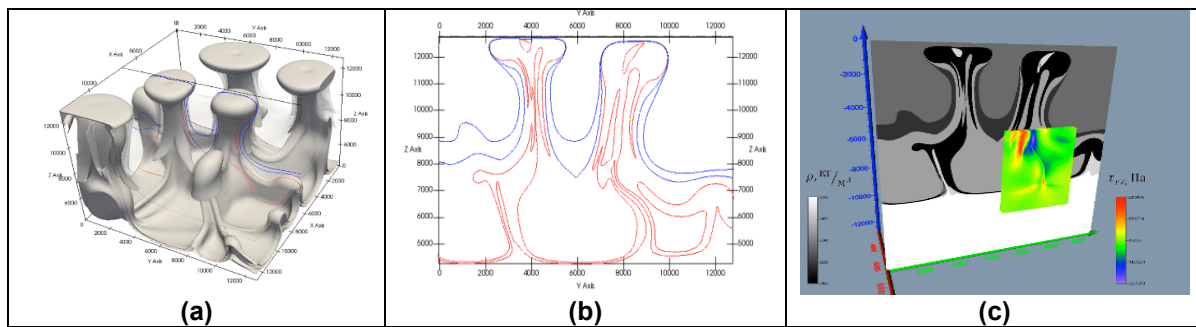


Figure 4 - (a) calculated state of the model, (b) cross-section of the 3d-model: red and blue colors show the boundaries of two unstable layers (density of the bottom layer is less than the top one), (c) details of the cross-section with calculated shear stress field τ_{yz} .